

Direct Torque Control of Induction Machines Using Space Vector Modulation

Thomas G. Habetler, *Member, IEEE*, Francesco Profumo, *Senior Member, IEEE*, Michele Pastorelli, and Leon M. Tolbert, *Member, IEEE*

Abstract—This paper describes a control scheme for direct torque and flux control of induction machines based on the stator flux field-orientation method. With the proposed predictive control scheme, an inverter duty cycle has directly calculated each fixed switching period based on the torque and flux errors, the transient reactance of the machine, and an estimated value of the voltage behind the transient reactance. The paper describes a method by which a voltage space vector can be calculated in order to control the torque and flux directly in a deadbeat fashion. The inverter duty cycle can then be calculated using the space vector PWM technique. With this scheme, the requirement of a separate current regulator and proportional-integral (PI) control of the flux, torque, and/or current error is eliminated, thereby improving transient performance. An alternative modulation scheme is presented in which transient performance is improved by specifying the inverter switching states *a priori*, then calculating the required switching instants to maintain deadbeat control of the flux while reducing the torque error during the entire switching interval. A similar approach is used for a transient in the flux. The implementation of the control scheme using DSP-based hardware is described, with complete experimental results given.

INTRODUCTION

IN MANY VARIABLE-speed drive applications, torque control is required or desired, but precise, closed-loop control of speed is not necessary. The advantages of torque control in this type of application include greatly improved transient response, avoidance of nuisance over-current trips, and the elimination of load-dependent controller parameters. An example of an application where torque is to be controlled, without precise speed control, is traction drives for electric vehicles. Here, the torque command comes directly from the user input. Speed control, if used at all, needs not be precise. In traction applications, as well as applications that currently use open-loop, constant V/f drives, a torque control scheme

that does not require motor speed information is very advantageous.

Stator flux field orientation (SFO) [1], [2] has gained interest as an induction machine torque control scheme due to the fact that speed feedback is not required to control the torque produced by the machine. The flux and torque are calculated (estimated) from the stator voltage, current, and resistance. A torque-producing component of current and a flux-producing component of current can be identified without knowledge of the rotor speed, position, or flux.

SFO drives typically derive a stator current command in the stationary dq reference frame based on the calculated torque and flux error. A current regulator is then used to generate the appropriate gating signals to the inverter. This scheme, however, requires a decoupling of the torque-producing component of current and the stator flux.

The problem of decoupling the stator current in a dynamic fashion can be avoided. Reference [3] presents a method of stator flux orientation in which the torque and flux errors are directly sent through proportional-integral (PI) regulators to generate a dq voltage reference. A voltage space vector PWM scheme [6] is then used to control the inverter. The transient response of this torque control method is still limited by the PI regulators in both the torque and flux loops.

The method of direct self control [4], [5] was introduced to control the torque and flux directly based solely on the instantaneous errors in torque and flux. This method is very well suited to high-power drives with low switching frequency. The inverter is switched in a hysteresis (or band-bang) fashion based directly on the torque and flux in the machine. This method, however, results in a variable switching frequency due to the hysteresis control.

The scheme proposed in this paper is also based on direct control of the torque and flux but has the advantage of a fixed switching period. Like the other direct torque controlled schemes, no inner current regulation loop is used. The proposed scheme calculates the inverter switching pattern (i.e., duty cycle) *directly* in order to control the torque and flux in a deadbeat fashion over a constant switching period. This is accomplished by calculating the voltage space vector required to control the

Paper IPCSD 92-12, approved by the Industrial Drives Committee of the IEEE Industry Applications Society for presentation at the 1991 Industry Applications Society Annual Meeting, Dearborn, MI, September 28–October 4. Manuscript released for publication March 1, 1992.

T. G. Habetler is with the School of Electrical Engineering, Georgia Institute of Technology, Atlanta, GA 30332.

F. Profumo and M. Pastorelli are with the Dipartimento di Elettrotecnica, Politecnico di Torino, Torino, Italy.

L. M. Tolbert is with Martin Marietta Energy Systems, Oak Ridge National Laboratory, Oak Ridge, TN 37831.

IEEE Log Number 9203303.

torque and flux on a cycle-by-cycle basis using the calculated flux and torque errors sampled from the previous cycle and an estimate of the back EMF in the machine. The back EMF of the machine is estimated from the flux and voltage vectors, which are already-available quantities in the SFO controller. Voltage space vector PWM is then used to find the switching intervals (duty cycle). An alternative control method is used under transient conditions since the space vector PWM does not yield a solution when the torque and/or the flux cannot be driven to the reference value in a single switching period. A block diagram of the direct torque controlled drive is shown in Fig. 1.

ESTIMATION OF MOTOR QUANTITIES

It is convenient in SFO drives to convert the system quantities to a stationary, two phase dq reference frame. An arbitrary three-phase quantity f_a, f_b, f_c can be transformed to the stationary dq reference frame by

$$\bar{f} = f_d + jf_q = f_a + j\left(\frac{f_a + 2f_b}{\sqrt{3}}\right). \quad (1)$$

The stator flux dq vector is determined from the stator voltage vector \bar{V}_s , the stator resistance R_s , and the stator current vector \bar{I}_s by

$$\bar{\lambda}_s = \int_0^t (\bar{V}_s - \bar{I}_s R_s) d\tau. \quad (2)$$

As is the case with any SFO drive scheme, the calculation of the stator flux requires knowledge of the stator resistance, particularly at low speed below about 5 Hz. Therefore, the speed range of the drive is limited unless some form of resistance estimator or tuning is incorporated.

The electromagnetic torque produced by the machine can be written in terms of the stator current and flux as

$$T = \frac{3}{2} \frac{p}{2} (\bar{\lambda}_s \times \bar{I}_s) = \frac{3}{2} \frac{p}{2} (\lambda_{ds} I_{qs} - \lambda_{qs} I_{ds}) \quad (3)$$

where p is the number of poles in the machine. An equivalent circuit in the stationary reference frame of the inverter-driven induction machine is shown in Fig. 2. From Fig. 2, the change in stator current vector $\Delta \bar{I}_s$ over a constant period T_s is given by

$$\Delta \bar{I}_s = \frac{\bar{V} - \bar{E}}{L'_s} T_s. \quad (4)$$

The period T_s is constant in the proposed scheme in order to maintain a constant switching frequency. At speeds above a few Hertz, the stator IR drop can be neglected, in which case \bar{V}^* is equal to \bar{V}_s^* . It is assumed that the stator electrical time constant is much longer than T_s , and therefore, the change in current over the period T_s is linear. The corresponding change in electromagnetic torque over the period T_s is then

$$\Delta T = \frac{3}{2} \frac{p}{2} (\bar{\lambda}_s \times \Delta \bar{I}_s) = \frac{3}{2} \frac{p}{2} \left(\bar{\lambda}_s \times \frac{\bar{V}_s - \bar{E}}{L'_s} T_s \right). \quad (5)$$

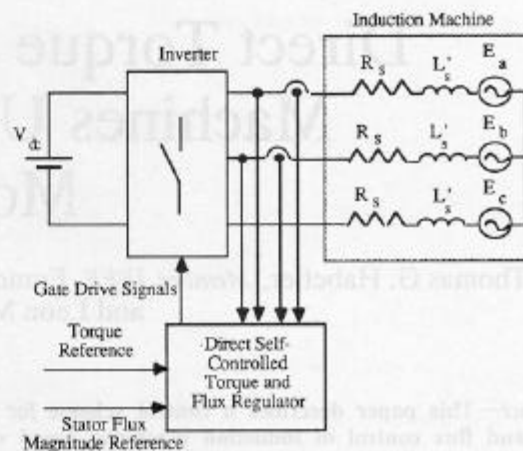


Fig. 1. Block schematic of direct torque and flux controlled induction machine drive.

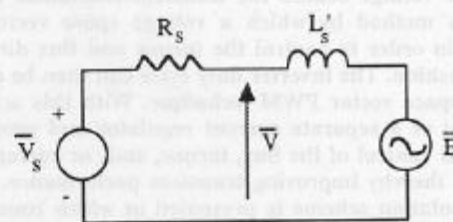


Fig. 2. Equivalent circuit of inverter-driven induction machine in the dq stationary reference frame.

Therefore, the change in torque over a period can be predicted from the stator voltage and current and the voltage behind the transient reactance \bar{E} . This voltage can be estimated from the stator flux and current. Using (2) and the dq equivalent circuit of the induction machine drive system shown in Fig. 2, the voltage behind the transient reactance is

$$\bar{E} = \bar{V}_s - R_s \bar{I}_s - \frac{d}{dt} (L'_s \bar{I}_s) = \frac{d}{dt} (\bar{\lambda}_s - L'_s \bar{I}_s). \quad (6)$$

If it is assumed that \bar{E} is sinusoidal, then

$$\bar{E} = j\omega_e (\bar{\lambda}_s - L'_s \bar{I}_s). \quad (7)$$

The excitation frequency ω_e in (7) can be estimated using the stator flux vector and the terminal quantities, as in [3]. In order to find the average stator frequency, it is assumed that $\bar{\lambda}_s$ is sinusoidal, then

$$\omega_e = \frac{\bar{\lambda}_s \times j\omega_e \bar{\lambda}_s}{|\bar{\lambda}_s|^2} = \frac{\bar{\lambda}_s \times (\bar{V}_s - R_s \bar{I}_s)}{|\bar{\lambda}_s|^2}. \quad (8)$$

Therefore, the change in torque over the period T_s can be found from (5)–(8). The change in flux over some period T_s is simply given by

$$\Delta \lambda_s = (\bar{V}_s - R_s \bar{I}_s) T_s = \bar{V} T_s. \quad (9)$$

The control scheme described in the next section uses the estimated or predicted values of the change in flux and

torque ((5) and (9)) to determine the switching state of the inverter.

DEADBEAT TORQUE AND FLUX CONTROL

The proposed control scheme is based on a predictive calculation of the stator voltage vector, which will drive the torque and flux magnitude to the reference value in a deadbeat fashion over a constant period. A fixed time period equal to half the switching period is denoted by T_s . Let t_n be the time at the beginning of an arbitrary T_s period. The torque is controlled in a beat manner if, over the T_s period

$$\Delta T = T^* - T(t_n) \quad (10)$$

where T^* is the reference or command value of torque. Equation (10) is then substituted into (5) to yield

$$T^* - T(t_n) = \frac{3}{2} \frac{p}{2} \frac{T_s}{L'_s} (\bar{\lambda}_s \times (\bar{V}^* - \bar{E})) \quad (11)$$

where \bar{V}^* is the voltage vector (minus the stator IR drop), which results in deadbeat control of the torque. In terms of d and q components

$$\Delta T = \frac{3pT_s}{4L'_s} ((-\lambda_{ds}E_q + \lambda_{qs}E_d) + (\lambda_{ds}V_q^* - \lambda_{qs}V_d^*)), \quad (12)$$

Let K_e be defined as

$$K_e = \frac{4\Delta TL'_s}{3pT_s} + (\lambda_{ds}E_q - \lambda_{qs}E_d). \quad (13)$$

Then, the q component of voltage is

$$V_q^* = \frac{K_e + \lambda_{qs}V_d^*}{\lambda_{ds}}. \quad (14)$$

The stator flux magnitude is controlled such that

$$\Delta|\bar{\lambda}| = \lambda_s^* - |\bar{\lambda}(t_n)| \quad (15)$$

where λ_s^* is the command value of stator flux magnitude. Using (9), the voltage \bar{V}^* required for deadbeat control of the flux magnitude is found from

$$\lambda_s^* = |\bar{V}T_s + \bar{\lambda}_s(t_n)| \quad (16)$$

or

$$\lambda_s^{*2} = (V_q^*T_s + \lambda_{qs})^2 + (V_d^*T_s + \lambda_{ds})^2 \quad (17)$$

where $\bar{\lambda}_s$ is assumed to be the value of flux vector at the beginning of the period T_s . Equations (11) and (17) represent two equations with two unknowns V_q^* and V_d^* . Substituting (14) into (17) gives a quadratic equation with V_d^*

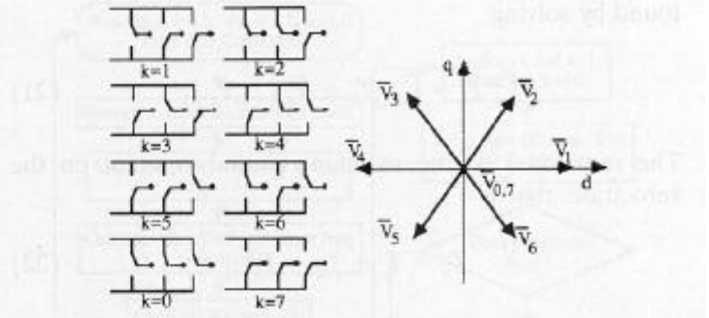


Fig. 3. Inverter switching states and stator voltage vectors.

as the unknown.

$$\begin{aligned} & \left(T_s^2 + \frac{\lambda_{qs}^2}{\lambda_{ds}^2} T_s^2 \right) V_d^{*2} \\ & + \left(\frac{2K_e\lambda_{qs}T_s^2}{\lambda_{ds}^2} + 2\lambda_{ds}T_s + \frac{2\lambda_{qs}^2T_s}{\lambda_{ds}} \right) V_d^* + \frac{T_s^2K_e^2}{\lambda_{ds}^2} \\ & + \frac{2\lambda_{qs}K_eT_s}{\lambda_{ds}} + \lambda_{ds}^2 + \lambda_{qs}^2 - \lambda_s^{*2} = 0. \end{aligned} \quad (18)$$

Equation (18) yields two solutions for V_d^* . The solution with the smallest absolute value is chosen since it represents the smallest d -axis voltage necessary to drive the torque and flux to their reference values. Equation (14) then gives V_q^* . Once \bar{V}^* is found from (18), the reference value of stator voltage is obtained by adding on the stator IR drop, that is

$$\bar{V}_s^* = \bar{V}^* + R_s \bar{I}_s(t_n). \quad (19)$$

Note that in (19), the stator IR drop from the previous cycle is added to \bar{V}^* . As stated earlier, the change in stator current is assumed to be linear since the stator IR drop is very small compared with the voltage drop across L'_s . In addition, (19) is justified since the change in stator current vector over T_s is very small compared with the magnitude of the stator current vector.

The switching state of the inverter is determined from \bar{V}_s^* using space vector PWM [6]. \bar{V}_s^* represents the average value of the stator voltage vector over the period T_s . The instantaneous stator voltage vector \bar{V}_s takes on one of seven values depending on the switching state k of the inverter. This is depicted in Fig. 3. The stator voltage is given by

$$\bar{V}_{s(k)} = \begin{cases} \frac{2}{3} V_{dc} e^{j(k-1)\pi/3} & k = 1, 2, \dots, 6 \\ 0 & k = 0, 7. \end{cases} \quad (20)$$

The reference voltage is realized in an average sense by computing the duty ratio (fraction of the switching period) for the two voltage vectors $\bar{V}_{s(k)}$ and $\bar{V}_{s(k+1)}$, which are adjacent to \bar{V}_s^* . Let T_k and T_{k+1} be amount of time spent on $\bar{V}_{s(k)}$ and $\bar{V}_{s(k+1)}$, respectively. Then, T_k and T_{k+1} are

found by solving

$$\bar{V}_s^* T_s = \bar{V}_{s(k)} T_k + \bar{V}_{s(k+1)} T_{k+1} \quad (21)$$

The remainder of the switching period is spent on the zero state, that is

$$T_0 = T_s - T_k - T_{k+1} \quad (22)$$

where T_0 is the time spent on the zero state ($k = 0$ or 7). Switching from the zero state to two adjacent states involves commutating each of the inverter legs exactly once. Therefore, T_s is a half period of the switching frequency. This implies that the torque and flux are controlled twice per switching cycle. In addition, the space vector PWM results in reduced current ripple in steady-state operation as compared with sine-triangle PWM current regulator-based controllers [6], [7].

TORQUE AND FLUX CONTROL UNDER TRANSIENT CONDITIONS

It is important to maximize the dynamic response to transients in the torque and/or flux command. With a sufficiently large torque error in one switching period, such as that which occurs with a step change in flux command, the simultaneous solution of (21) and (22) yields the sum $T_k + T_{k+1}$ greater than T_s , that is, \bar{V}_s^* is too large to be synthesized in a single switching period. Therefore, an alternative control method must be derived. In the case of a transient in the torque command, the controller must cause the torque to be driven toward its reference value while still maintaining deadbeat control of the flux. Just the opposite is true in the case of a flux reference transient. Then, the flux magnitude is driven toward the reference value while maintaining deadbeat control of the torque.

Consider first the case of a transient condition in the torque, that is, the torque cannot be driven to the reference value in a single T_s period. This is generally the most important and most frequently encountered transient condition. In this case, the inverter states are chosen *a priori*, which causes the torque to be driven in the desired direction while still allowing for deadbeat control of the flux. To illustrate this state selection, consider an example where the angle of the flux vector is between $-\pi/6$ and $+\pi/6$. This is illustrated in the vector diagram of Fig. 4. States 2 and 3 cause the current in quadrature with the stator flux, and therefore the torque, to increase. Likewise, states 5 and 6 cause the torque to decrease. In addition, from Figs. 3 and 4, states 2 and 6 cause the flux magnitude to increase, and states 3 and 5 cause the flux magnitude to decrease. Therefore, states 2 and 3 can be used to control the flux to its reference value over the T_s interval while continuously increasing the torque over the entire interval. Table I summarizes the state selection for a transient in the torque command. Once the states k and $k+1$ are identified, the flux is controlled by substituting

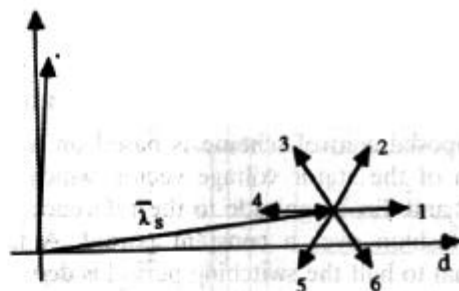


Fig. 4. Vector diagram illustrating the state selection process for transient operation.

TABLE I
SELECTION OF INVERTER STATES k AND $k+1$ UNDER TRANSIENT CONDITIONS

$(2n-3)\frac{\pi}{6} < \text{angle } \bar{\lambda}_s < (2n-1)\frac{\pi}{6}$ (a) Torque Transient		
$\text{Sgn}(T - T^*)$	k	$k+1$
$\text{Sgn}(\lambda_s - \lambda_s^*)$	k	$k+1$
$\text{Sgn}(T - T^*)$	k	$k+1$
		$n+1$
		$n+2$
		$n+4$
		$n+5$

\bar{V}_k and \bar{V}_{k+1} into (16), that is

$$\lambda_s^* = |\bar{V}_{s(k)} T_k + \bar{V}_{s(k+1)} T_{k+1} + \bar{\lambda}_s(t_n)| \quad (23)$$

Since it is desired to drive the torque in one direction as quickly as possible, the zero state is not used under transient conditions. Therefore

$$T_s = T_k + T_{k+1} \quad (24)$$

Equations (23) and (24) are solved simultaneously for T_k and T_{k+1} . In this way, the flux is controlled to its reference value, and the torque is driven continuously in the proper direction with maximum voltage applied to the machine.

Now, consider the case of a transient in the flux command, that is, the flux magnitude cannot be driven to the reference value in a single T_s period. In this case, the state selection is again made *a priori*. Using the above example (Fig. 4), states 1 and 2 both increase flux, and states 3 and 4 both decrease the flux. The determination of k and $k+1$ for controlling the torque while during a flux transient is also given in Table I. The torque is controlled by substituting V_k and V_{k+1} into (11), that is

$$\Delta T = \frac{3}{2} \frac{p}{2} \frac{1}{L_s} (\bar{\lambda}_s \times (\bar{V}_k T_k + \bar{V}_{k+1} T_{k+1} - \bar{E} T_s)) \quad (25)$$

Equation (25) is solved simultaneously with (24) for T_k and T_{k+1} . This accomplishes the deadbeat control of the torque while driving the flux in the desired direction. Here, again, the zero state is not used. This is perfectly reasonable since skipping the zero state while still switching between adjacent states is equivalent to pulse dropping in conventional sinusoidal modulation.

The only remaining possibility is a transient in both the torque and the flux. In this case, a single state is selected for the entire period, which drives both the torque and flux in the desired directions as quickly as possible. The state selection is given in Table I. The selected states cause both the torque and flux to be driven in the proper direction. Selecting a single state for the entire T_s period is essentially pulse dropping on all three phases (six-step operation).

REALIZATION AND SIMULATION OF THE CONTROL SCHEME

The realization of the direct torque control scheme is outlined in the flowchart in Fig. 5. The switching states of the inverter and the corresponding dwell times are determined each half switching period. The controller reads in the stator voltage and current at the beginning of a particular switching period. The stator flux is then calculated. In the actual implementation done here, analog hardware is used to find the stator flux due to the ease of performing analog integration, thereby relieving the microprocessor from this duty. Details of the experimental hardware are given in the next section. It is assumed in this paper that the stator resistance and transient reactance are known quantities. The stator flux and torque are then used to calculate the present value of torque and synchronous speed. The back EMF of the machine is then calculated from the speed, flux, and current.

Equation (18) is then solved for V_d^* using the quadratic formula. The square root is found using a Taylor series expansion. The Taylor series expansion is done about the previous interval's solution. In this way, it has been found that only three terms in the expansion yield a solution with less than 5% error. Using a truncated Taylor series expansion with a good initial estimate of the solution allows (18) to be solved within a very reasonable computational time.

The two inverter states adjacent to \bar{V}^* are then found, and finally, the switching intervals are found by solving (21) and (22). If a positive solution does not exist, then a transient condition is encountered. In this case, it is first assumed that a transient exists in the torque command. Table I(a) is used to determine the adjacent inverter states, and then, (23) and (24) are solved. If a positive solution for T_k and T_{k+1} does not exist, then (24) and (25) are solved using the states given in Table I(b). If a solution still does not exist, the inverter is switched to the state indicated in Table I(c).

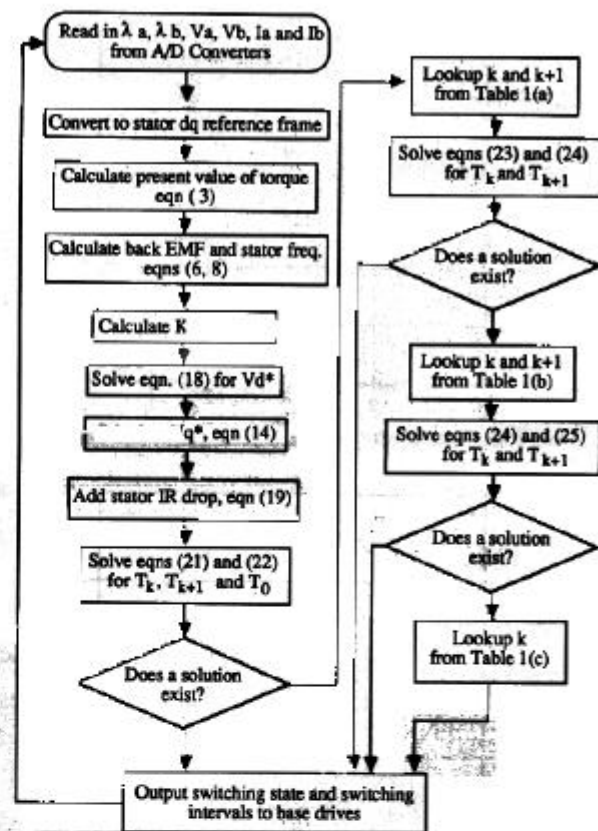


Fig. 5. Flowchart of direct torque control scheme.

As with any predictive control scheme, as this one is, a single T_s period steady-state error exists since the torque and flux calculations are based on input data from the *preceding* period. A one-period delay is necessary to allow time to calculate the switching pattern. An ideal deadbeat controller would require the calculations to be done in zero time. Furthermore, the controller is based solely on instantaneous errors in the torque and flux. This fact, combined with the one-period delay, results in a steady-state error in the commanded torque. If the torque regulator is used together with an outer speed control loop, this does not present a problem. However, if the steady-state error in the torque is not tolerable, an outer loop that adjusts the torque reference based on the average error (i.e., the integral of the torque error) can be added. It is important to note that this additional outer loop in no way compromises the dynamic performance of the direct-torque controller.

The proposed control system is implemented using a digital signal processor (DSP) to perform the requisite calculations. The DSP, which is characterized by hardware multiplication capability, allows for a large number of arithmetic operations to be performed during each T_s period. The transient control scheme in addition to the aforementioned deadbeat control increases the computational burden quite significantly. This is not a problem with a relatively low switching frequency (in this case, 2 kHz). However, at higher switching frequencies, depending on the speed of the processor and the A/D convert-

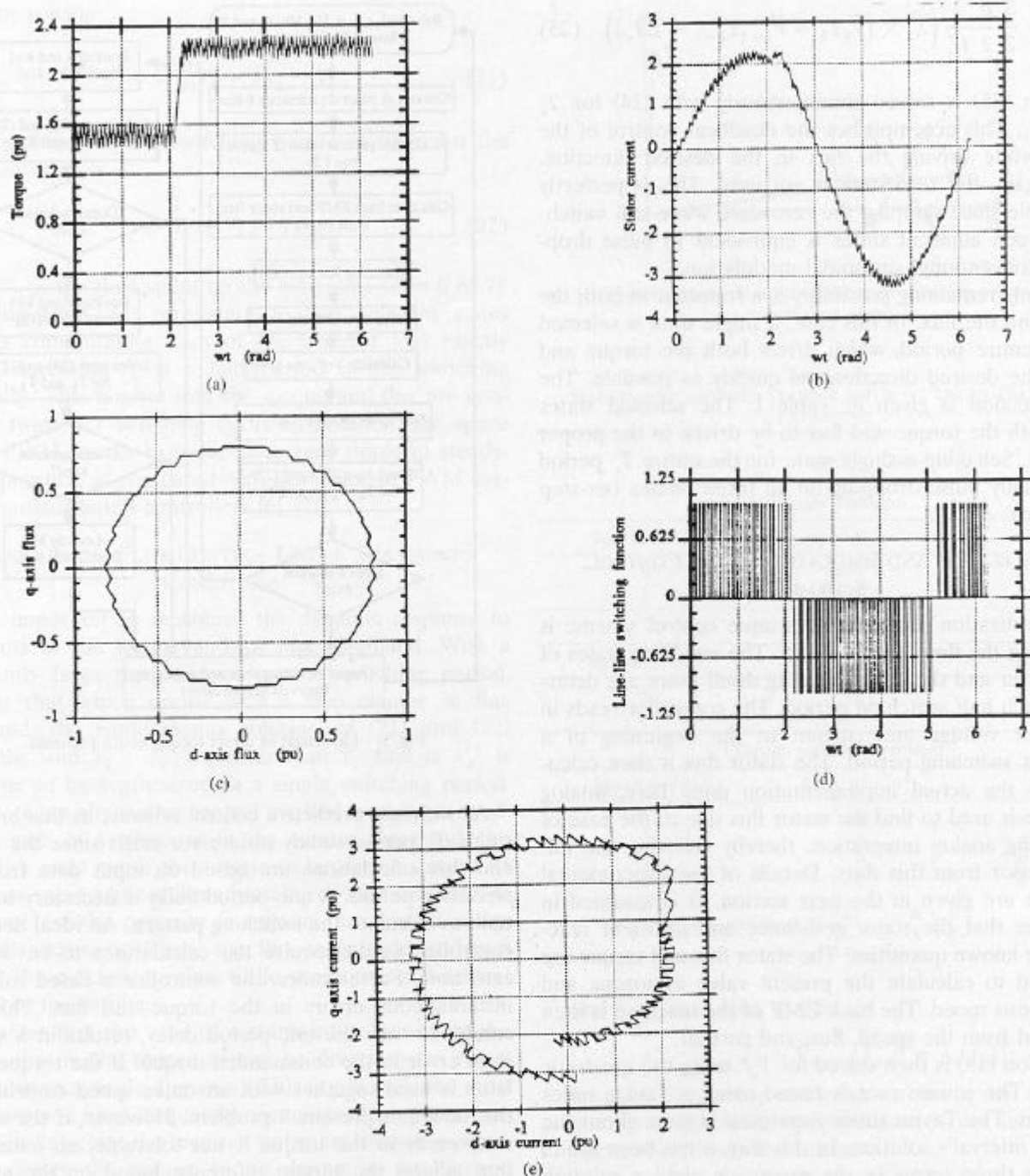


Fig. 6. Simulation results: (a) Electromagnetic torque; (b) stator line current; (c) stator flux; (d) line-line switching function; (e) stator current vector.

ers, sufficient time may not be available to implement the transient computations. In this case, the stator voltage can be set equal to a voltage proportional to the calculated V^* by setting the actual inverter switching times T'_k and T'_{k+1} equal to

$$T'_k = T_k \frac{T_s}{T_k + T_{k+1}} \quad \text{and} \quad T'_{k+1} = T_{k+1} \frac{T_s}{T_k + T_{k+1}}. \quad (26)$$

This method results in satisfactory performance but does not give deadbeat control under transient conditions.

This is due to the fact that the zero state is not used, and therefore, (22) is not satisfied.

The simulation results are shown in Fig. 6. The switching frequency is 2 kHz, the transient reactance is 0.14 pu at 60 Hz, and the dc bus voltage is 3.0 pu. The flux reference is 0.8 pu. The simulation results illustrate both the steady-state and transient performance of the proposed torque control scheme. Note the good dynamic response of the system to a step change in torque command. It is also clear from Fig. 7(c) that the flux regulation is quite good, even during the torque transient.

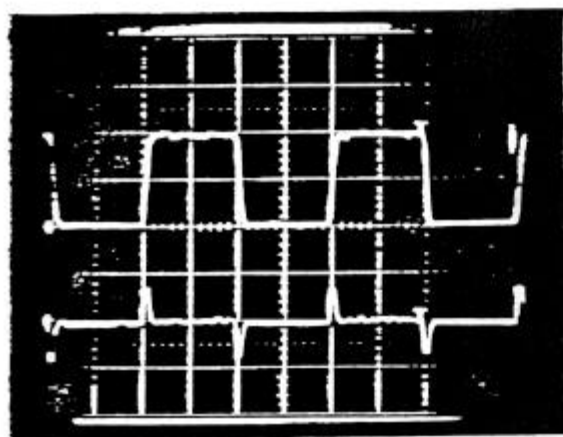


Fig. 7. Experimental waveforms. Top trace: mechanical speed, 600 r/min/div. Bottom trace: estimated torque, 210 N·m/div. Horiz: 10 ms/div.

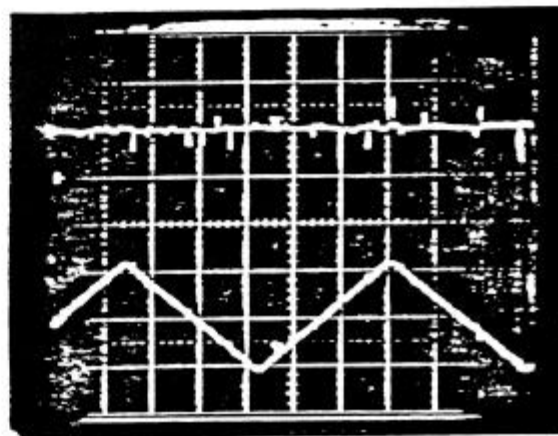


Fig. 8. Experimental waveforms. Top trace: estimated flux magnitude, 1 V·s/div. Bottom trace: mechanical speed, 600 r/min/div. Horiz: 200 ms/div.

EXPERIMENTAL RESULTS

The experimental setup includes a complete motor drive consisting of a three-phase bipolar inverter with a switching frequency of 2 kHz and a 15-hp induction motor. The main switches are rated at 1000 V and 200 A. The complete control scheme, including the space vector PWM, is performed by a single TMS 32010 digital signal processor that has only 4 k of memory. The total time available to read in the data, execute the software, and output the switching state to the inverter is $T_s = 250 \mu\text{s}$. The steady-state control scheme (without the transient computations) consumes approximately $150 \mu\text{s}$. This includes $10 \mu\text{s}$, minimum, for A/D conversion. The complete control scheme, including transient operation, can be easily implemented within the $250\text{-}\mu\text{s}$ period. It should also be noted that the actual software has not been optimized in any way for speed and that significant improvements in computing time could be realized by fully utilizing the high level of pipelining available in the DSP.

As stated earlier, the stator flux is calculated using simple analog integrator. The line-neutral voltages used to determine the flux are found from the dc bus voltage and the inverter switching state. The space vector-based controller is very convenient to implement in digital software since no digital-to-analog converters are required, as is the case with sine-triangle PWM controllers. The experimental controller uses a tachometer speed feedback to generate the torque reference. The speed error is sent through a PI controller, which gives the torque reference.

The experimental results are shown in Figs. 7–11. Various tests have been carried out to characterize the performance of the proposed control system. First, a speed reference alternating between ± 300 r/min is applied to the system. The response of the controller is shown in Fig. 7. The bottom trace shows the calculated torque readout from the controller through a D/A converter. It can be seen from the oscillogram that the torque regulation is quite good. In Fig. 8, the stator flux magnitude is depicted. Note the stator flux magnitude remains constant even with large changes in the speed (torque). Fig. 9 shows the

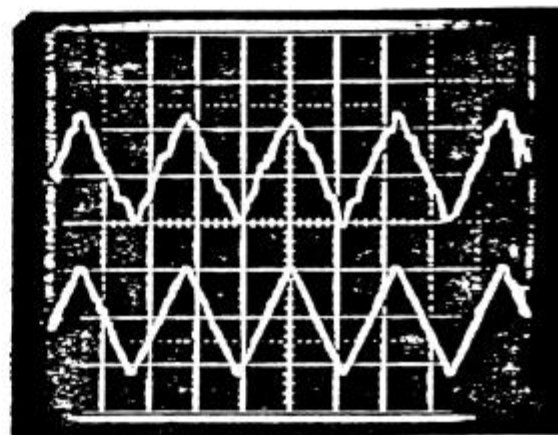


Fig. 9. Experimental waveforms. Top trace: estimated synchronous frequency, 125.6 rad/s/div. Bottom trace: mechanical speed, 600 r/min/div. Horiz: 500 ms/div.

output of the synchronous speed estimator in comparison with the actual motor speed. In Fig. 10, the estimated d -axis flux is shown with a large change in the speed. Finally, Fig. 11 shows the stator line current in the steady state.

CONCLUSIONS

This paper has presented a direct induction machine torque control method based on predictive, deadbeat control of the torque and flux. By estimating the synchronous speed and the voltage behind the transient reactance, the change in torque and flux over the switching period is calculated. The stator voltage required to cause the torque and flux to be equal to their respective reference values is calculated. Space vector PWM is then used to define the inverter switching state. An alternative approach to dead-beat control was also presented for use in the transient or pulse-dropping mode.

This type of torque control has several advantages. First, the torque and flux are controlled twice per switching period. Therefore, the steady-state delay, which is

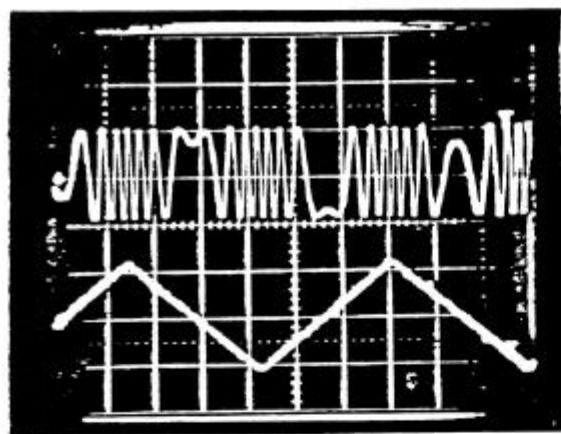


Fig. 10. Experimental waveforms. Top trace: estimated d -axis stator flux, $1 \text{ V} \cdot \text{s}/\text{div}$. Bottom trace: mechanical speed, $600 \text{ r/min}/\text{div}$. Horiz: $200 \text{ ms}/\text{div}$.

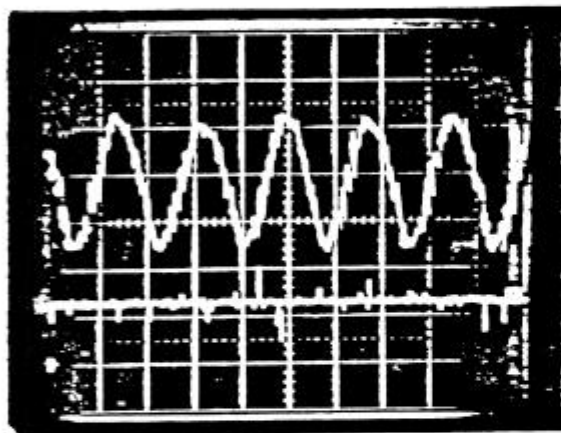


Fig. 11. Experimental waveforms. Top trace: stator line current, $15 \text{ A}/\text{div}$. Bottom trace: speed reference, $300 \text{ r/min}/\text{div}$. Horiz: $50 \text{ ms}/\text{div}$.

present in any predictive scheme, is only equal to half the switching period. Second, the space vector PWM results in reduced line current ripple in comparison with sine-triangle PWM-based controllers. The direct torque control scheme results in very good performance without the requirement for speed feedback. The estimation of the machine back EMF allows the controller to accurately predict the change in torque over the switching period. This type of predictive control scheme is superior to conventional current-regulated PWM torque controlled drives that are not based on a complete model of the machine, that is, the current is regulated without knowledge of the motor parameters. The back EMF estimator was shown to operate quite satisfactorily through both simulation and experimental results.

The scheme presented in this paper is certainly computationally intensive. However, with present microcomputer hardware, this control scheme is easily realized in software with a 2-kHz switching frequency, which is typical of hard-switched transistor inverters. The experimental results clearly demonstrated the feasibility of such a computationally intensive control scheme.

APPENDIX MOTOR DATA

The characteristics for the machine used in the simulation study and the experimental work is given below.

Rated output power	15 hp
Rated voltage	380 V
Rated current	21.6 A
Maximum torque	$205 \text{ N} \cdot \text{m}$
Poles	4
Rated speed	1430 r/min
Max speed	3000 r/min
Stator resistance	0.371Ω
Rotor resistance	0.415Ω
Stator leakage inductance	2.72 mH
Rotor leakage inductance	3.3 mH
Mutual inductance	84.33 mH

REFERENCES

- [1] X. Xu, R. DeDoncker, and D. W. Novotny, "A stator flux oriented induction machine drive," in *PESC 1988 Conf. Rec.*, pp. 870-876.
- [2] —, "Stator flux orientation control of induction machines in the field weakening region," in *IEEE-LAS Conf. Rec.*, 1988, pp. 437-443.
- [3] X. Xue, X. Xu, T. G. Habetler, and D. M. Divan, "A low cost stator flux oriented voltage source variable speed drive," in *IEEE-LAS Ann. Mtg. Conf. Rec.*, 1990, pp. 410-415.
- [4] M. Depenbrock, "Direct self control (DSC) of inverter-fed induction machines," *IEEE Trans. Power Electron.*, vol. 3, no. 4, pp. 420-429, Oct. 1988.
- [5] I. Takahashi and T. Noguchi, "A new quick-response and high-efficiency control strategy of an induction motor," *IEEE Trans. Industry Applications*, vol. IA-22, no. 5, pp. 820-827, 1986.
- [6] H. W. van der Broeck, H. C. Skudelny, and G. Stanke, "Analysis and realization of a pulse width modulator based on voltage space vectors," in *IEEE-LAS Conf. Rec.*, 1986, pp. 244-251.
- [7] T. G. Habetler, "A space vector-based rectifier regulator for ac/dc/ac converters," in *Proc. Euro. Power Electron. Conf.*, 1991.
- [8] I. Boldea and S. A. Nasar, "Torque vector control—A class of fast and robust torque/speed and position digital controllers for electric drives," *Elec. Machines Power Syst. J.*, vol. 15, pp. 135-147, 1988.
- [9] I. Boldea and J. A. Trica, "Torque vector controlled (TVC) voltage-fed induction motor drives—Very low speed performance via sliding mode control," in *Proc. Int. Conf. Elec. Machines*, 1990, pp. 1212-1217, pt. 3.



Thomas G. Habetler (S'82-M'83-S'85-M'89) received the B.S.E.E. degree in 1981 and the M.S. degree in 1984, both in electrical engineering, from Marquette University, Milwaukee, WI, and the Ph.D. degree from the University of Wisconsin-Madison, in 1989.

From 1983-1985, he was employed by the Electro-Motive Division of General Motors as a Project Engineer. While there, he was involved in the design of switching power supplies and voltage regulators for locomotive applications.

In 1985, he was awarded the General Motors Fellowship to attend the University of Wisconsin-Madison. He is currently an Assistant Professor of Electrical Engineering at the Georgia Institute of Technology. His research interests are in switching converter technology and electric machine drives.

Dr. Habetler was co-recipient of the 1989 First-Prize Paper Award and the 1991 Second-Prize Paper Award of the Industrial Drives Committee of the IEEE Industry Applications Society. He is chair of the Membership and Publicity Committee of the IEEE Power Electronics Society and is a member of the IEEE-IAS Industrial Power Converter and Industrial Drives Committees.



Francesco Profumo (SM'90) was born in Savona, Italy, in 1953. He received the 'laurea' (with honors) in electrical engineering from the Politecnico di Torino, Italy, in 1977.

From 1978 to 1984, he worked as a Research and Development Senior Engineer for the Ansaldo Group, Genoa, Italy. He then joined the Department of Electrical Engineering of the Politecnico di Torino, where he is now an Associate Professor of electrical drives. He was Visiting Professor in the Department of Electrical and Computer Engineering of the University of Wisconsin-Madison, from 1986 to 1988. His fields of interest are power electronics conversion, integrated electronic/electromechanical design, high response speed servo drives, and applications of new power devices. He published more than 60 papers in technical journals and conference proceedings.

Dr. Profumo is the secretary of the IEEE-PELS/IES Italian Chapter, and he was the Secretariat of the EPE'91 Conference held in Florence, Italy, in September 1991. He is a Registered Professional Engineer in Italy.



Mr. Pastorelli is a Registered Professional Engineer in Italy.

Michele Pastorelli was born in Novara, Italy, in 1962. He received the degree in electrical engineering from the Politecnico di Torino, Italy, in 1987.

He joined the Department of Electrical Engineering of the Politecnico di Torino in 1988. He is working towards the Ph.D. degree in electrical engineering, and his fields of interest are power electronics and high-performance servo drives. He has published more than 10 papers in technical journals and conference proceedings.



Leon M. Tolbert (S'88-M'91) received the B.E.E. and the M.S. degrees in electrical engineering from the Georgia Institute of Technology, Atlanta, in 1989 and 1991, respectively.

He is currently employed by Martin Marietta Energy Systems at the Oak Ridge National Laboratory in Tennessee. His interests include control of electric machines and power electronics applications.